AIP | Applied Physics Letters

Plasmon-enhanced photoluminescence from bioconjugated gold nanoparticle and nanodiamond assembly

Y. L. Liu and K. W. Sun

Citation: Applied Physics Letters **98**, 153702 (2011); doi: 10.1063/1.3576852
View online: http://dx.doi.org/10.1063/1.3576852
View Table of Contents: http://scitation.aip.org/content/aip/journal/apl/98/15?ver=pdfcov
Published by the AIP Publishing

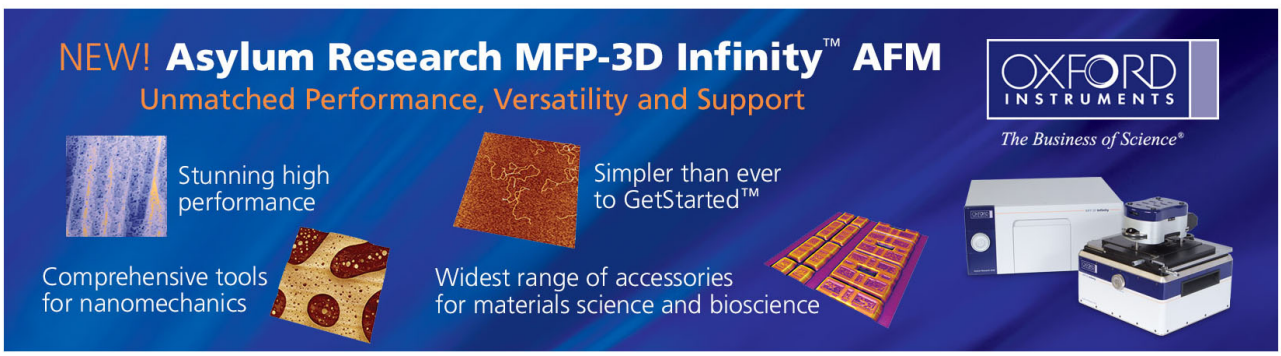

Plasmon-enhanced photoluminescence from bioconjugated gold nanoparticle and nanodiamond assembly

Y. L. Liu and K. W. Sun[a)]
Department of Applied Chemistry, National Chiao Tung University, Hsinchu 30010, Taiwan

(Received 6 November 2010; accepted 6 March 2011; published online 11 April 2011)

In this letter, we coupled nanodiamonds (NDs) with gold nanoparticles of different sizes using two complementary DNA sequences. After hybridizing the gold nanoparticles on the NDs, we observed the enhancement of the photoluminescence (PL) signals originating from the nitrogen-vacancy (N-V) center of the ND. The enhancement was attributed to the plasmon field created by the gold nanoparticles. The line shape of the enhanced PL spectra was also affected by the sizes of the attached nanoparticles due to their different resonant plasma frequencies. The signal enhancement can be used as an indexing tool for biosensing applications. © *2011 American Institute of Physics*. [doi:10.1063/1.3576852]

Metallic nanocrystals are known to enhance photoluminescence (PL) and Raman signals. The interactions between plasmonic metal nanocrystals and materials give rise to very interesting phenomenon, including fluorescence enhancement,[1,2] fluorescence quenching,[3,4] and molecular-plasma resonance.[5] The scattering properties and the plasma spectra of small gold nanoparticles make them behave as an elementary resonant dipole antenna. This near field enhancement has been exploited and employed to amplify surface-enhanced Raman scattering,[6] fluorescence,[7] photocurrent,[8] and light absorption.[9]

The optical properties of nanodiamonds (NDs) have been extensively investigated in recent years.[10,11] The major Raman peak of a diamond is located in 1332 cm^{-1}, and its band gap is 5.48 eV. Apart from the properties mentioned above, the photophysics of color centers in a diamond have attracted much interest because of their potential use for applications in quantum information processing and bioimaging. Nitrogen is the most prominently known impurity, which forms the nitrogen-vacancy (N-V) center in a diamond. The structure of the N-V center consists of a pair of substitutional nitrogen and vacancy. According to the impurities close to the surrounding area acting as electron donor or acceptor, the defects can form following two types of states: neutral N-V center $[(N\text{-}V)^0]$ and negatively charged N-V center $[(N\text{-}V)^-]$. A model for the neutral and charged N-V center in diamonds has been proposed and their corresponding absorption spectra have been fully discussed.[12,13]

Recently, the controlled coupling of a single N-V center in an ND to a gold nanoparticle via physical contact has been demonstrated using an atomic force microscope.[14] The emission properties of the N-V center have been controlled by coupling to the plasma resonance of the gold nanoparticle. In this letter, we demonstrated a gold nanoparticle-DNA-ND (Au-DNA-ND) hybrid structure to enhance the PL from the N-V centers in NDs. The enhanced PL intensities of the $(N\text{-}V)^0$ and $(N\text{-}V)^-$ states were affected by different plasma resonances of gold nanoparticles with various sizes.

Preparation of the ND-DNA1 solution, Au-DNA2 solution, and the final Au-DNA-ND hybrid structure was provided in the supplementary.[15] We performed continuous wave and time-resolved PL measurements for the above samples. A drop of properly diluted solution containing our hybrid structures was placed on a silicon substrate with patterned coordination markers.[10] A confocal microscope was used to allocate an isolated hybrid structure. The PL signals were collected through the microscope objective and are analyzed using a spectrometer equipped with a liquid nitrogen-cooled charge-coupled device (CCD) detector at the excitation wavelength of 488 nm. The excitation power density from the diode-pumped solid state (DPSS) laser was controlled under 10 KW/cm^2. The optical signal was further optimized by adjusting the focal plane position along the z-axis via the piezo-driven objective lens. For the time-resolved measurements, a pulsed diode laser was used as the excitation source at a wavelength of 405 nm; the pulse duration was 100 ps with a repetition rate of 10 MHz and an excitation density in the range of 1–100 W/cm^2. The time-resolved PL signal was analyzed with a 0.55 m spectrometer and detected by a microchannel photomultiplier with a time-correlated single-photon counting setup. The overall spectral resolution and system response were 0.1 meV and 300 ps, respectively.

Figure 1(a) shows the SEM image of the hybrid structures of NDs coupled with the 13 nm gold nanoparticles. Under the SEM images, nearly all of the gold nanoparticles were properly anchored on the NDs after the extra unbounded gold nanoparticles were washed away by centrifu-

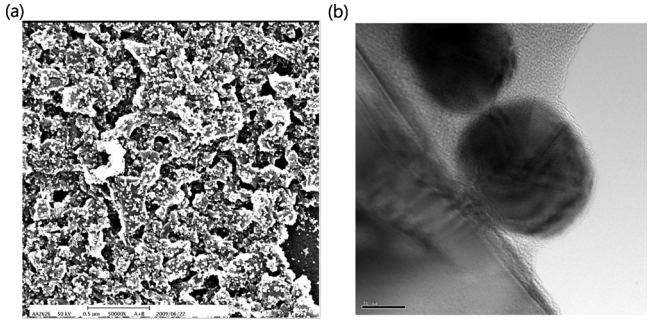

FIG. 1. (a) SEM image of Au-DNA-ND hybrid structures with 13 nm gold nanoparticles attached (b) HRTEM image of a 30 nm gold nanoparticle attached on a ND via a double string DNA.

a)Electronic mail: kwsun@mail.nctu.edu.tw.

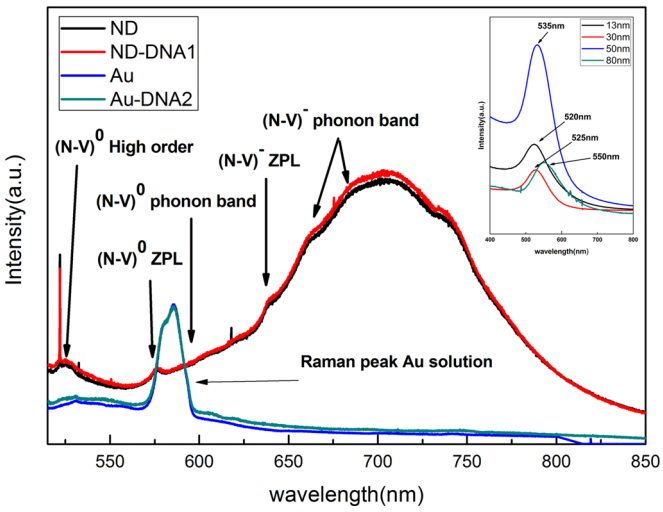

FIG. 2. (Color online) Photoluminescence spectra of bare ND, gold nanoparticles, Au-DNA2 assembly, and ND-DNA1 assembly. The inset shows absorption spectra of 13, 30, 50, and 80 nm Au nanoparticles.

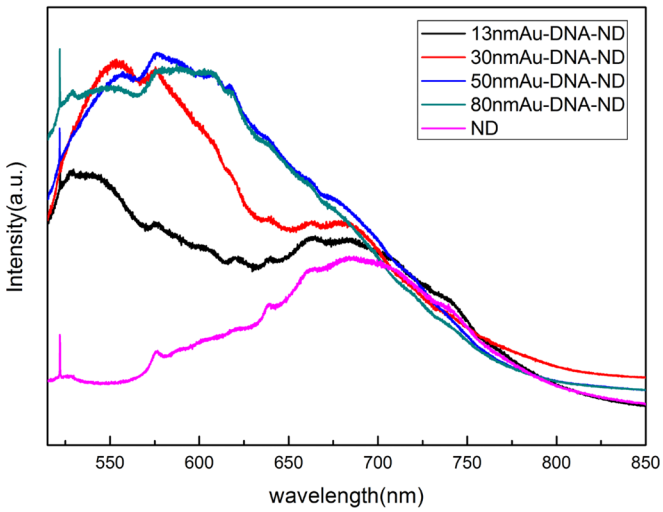

FIG. 3. (Color online) Plasmon enhanced photoluminescence spectra of Au-DNA-ND hybrid structures with gold nanoparticle sizes of 13, 30, 50, and 80.

gating for several times, indicating that the NDs were well bonded with the gold nanoparticles with the DNA linker. The bonding force was also strong enough to hold the hybrid structures during the centrifugation processes. Figure 1(b) shows the high-resolution transmission electron microscope (HRTEM) image of the 30 nm gold nanoparticle binding with an ND. Under this TEM image, the gold nanoparticle was completely placed on the top of the ND surface and there was no gap in between them, even though the DNA sequence had a length of 6 nm. After performing the test with a longer DNA sequence with a length of 20 nm (the results are not shown here), the TEM images also showed the close contact of the gold nanoparticle with the ND surface. There are several reasons that can explain our TEM results. The density of the carboxylated group on the ND surface was about 7%,[16,17] leading to the limited number of DNA linkers established on the ND surface. Due to the hydrophobic adsorption, DNA molecules that grafted onto the nanoparticle surface may be expected to stay flat.[18,19] Another explanation could be that the stiffness of DNA was about 10 pN/μm.[20] Due to the limited number of DNA sequences, they were not stiff enough to hold against the static attraction force in between the ND and gold nanoparticles. Therefore, the DNA sequences bended and allowed the gold nanoparticles to come in contact with the ND.

The luminescence properties of all tested nanoparticles were investigated individually before the coupling procedure was started. Figure 2 shows the luminescence properties of the NDs and 13 nm gold nanoparticles with and without coupling to a single string of DNA sequence at an excitation wavelength of 488 nm. In our experiments, optical excitation of gold nanoparticles showed a lack of or very weak luminescence. In an earlier report, the smooth gold films have a PL efficiency of only $\sim 10^{-10}$ following the excitation of electron from 5*d* to 6*sp* levels.[21] The poor luminescence efficiency can be attributed to the nonradiative energy relaxation processes of the photoexcited carriers, which is able to quench the PL. This could explain why the luminescence intensity of ~520 nm was undetectable for our gold nanoparticles; the peak that appeared at 590 nm was the Raman signal from the buffer solution. The luminescence spectrum of the NDs and the PL peak assignment are given in Fig. 2. The board emission band consisted of two zero phonon emissions and several phonon band replicas from $(N\text{-}V)^0$ and $(N\text{-}V)^-$.[11,12] The PL peaks at 575 and 638 nm originated from the $(N\text{-}V)^0$ and $(N\text{-}V)^-$ states,[22,23] respectively. Peaks that appeared at 596, 660, and 680 nm were divacancy-related phonon replica bands of the $(N\text{-}V)^0$ and $(N\text{-}V)^-$ states.[24,25] There was almost no change in luminescence intensity and line shape when the ND and gold nanoparticles were respectively coupled with DNA1 and DNA2 sequences. The plasmon resonance frequencies of our gold nanoparticles with sizes of 13, 30, 50, and 80 nm were determined to be at 520 nm, 525 nm, 535 nm, and 550 nm, respectively, according to the absorption spectra shown in the inset of Fig. 2.

In the next step, we begin our optical investigations on Au-DNA-ND hybrid structures. The hybrid structures coupled with different Au particle sizes were excited with a laser operated at 488 nm through a confocal microscope. The spectra of all four samples are plotted in Fig. 3. The PL spectra of pure NDs are also presented in parallel for comparison. We observed strong modification on the luminescence intensity profiles of the hybrid structures between 525–650 nm compared with the pure ND. In the case of 13 nm gold nanoparticles, the emission from the $(N\text{-}V)^0$ state was significantly enhanced than that from the $(N\text{-}V)^-$ state. This was due to the plasma resonance (~ at 520 nm) of 13 nm Au nanoparticles, which was closer to the emission energy of the $(N\text{-}V)^0$ state. Therefore, stronger enhancement on the PL intensity from the $(N\text{-}V)^0$ state emission was observed in smaller gold nanoparticles. As we increased the nanoparticles' sizes with their plasma resonances moving closer to the $(N\text{-}V)^-$ state emission, enhancement on the longer wavelength part of the PL was observed. Therefore, the profile of the enhanced PL could be altered depending on the sizes of the gold nanoparticles attached.

Our hybrid structures can be dissembled using a particular enzyme called restriction enzyme (NdeI). A NdeI cuts double-stranded or single-stranded DNA at specific recognition nucleotide sequences. If we let our hybrid structures interact with the NdeI, the link between the ND and gold nanoparticles can be disconnected. Therefore, the enhance-

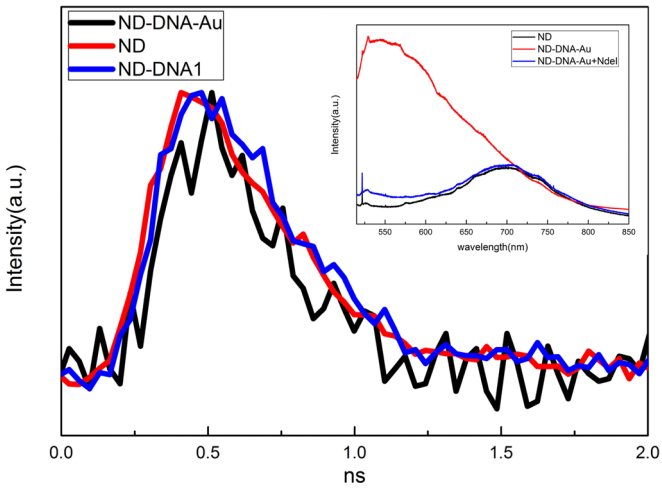

FIG. 4. (Color online) Time-resolved spectra of NDs, ND-DNA1 assembly, and Au-DNA-ND hybrid structures. The inset shows the PL spectra of ND, Au-DNA-Nd hybrid structures before and after interacting with NdeI restriction enzyme.

ment of PL should be deactivated because of the breaking of the DNA linkers. The PL spectra of our hybrid structures with the attached 13 nm gold nanoparticles removed by interacting with the NdeI is shown the inset of Fig. 4. Although our hybrid structures had a *p*H environment of 6.5, which did not match the restricting enzyme's ideal *p*H environment (the enzyme had a cutting rate of nearly 95% at *p*H=8.5 and at a temperature of 35 °C), the PL enhancement was strongly suppressed when the gold nanoparticles were detached from the NDs. This again proves that the enhanced PL is solely due to the plasmon resonance from the gold nanoparticles.

From time-resolved measurements, we obtained an excited state decay rate of the emission at 575 and 638 nm, corresponding to the emission maximum of the $(N\text{-}V)^0$ and $(N\text{-}V)^-$ states, respectively. The time-resolved spectra for the bare ND, ND bound with DNA1, and the hybrid structures bound with 13 nm Au nanoparticles are shown in Fig. 4. In contrast to the earlier reports,[14] we extracted a much faster decay time of ~0.38 ns for the bare ND at room temperature. The time-resolved spectrum of the ND-DNA1 was almost overlapped with that of the bare ND spectrum. However, for the hybrid structures, we obtained a slight increase in the excited state decay rate by a factor of 1.5, which was limited by the system response. The decay rate of the hybrid structures also showed no dependence on the size of the Au nanoparticle attached. The faster decay times observed in the luminescence were probably due to the shorter excitation wavelength used in our measurements. The PL of NDs was found to be size and laser excitation wavelength dependent[11] due to two competitive origins: the surface states[26,27] and vacancy centers in bulk diamond phase. When NDs are excited with short wavelengths, the radiation recombination will be affected by the surface states (or structural inhomogeneities). The ultrafast optical emission with a decay time of 60 ps in ultrafine NDs was reported under pulsed laser excitation of 300 nm.[26] It was attributed to the surface states and large surface-to-volume ratio of nanoparticles. We speculate that, with an excitation of 405 nm, carriers are excited in or above the surface defect states and have an effect on the radiative transitions and PL lifetimes from the vacancy centers. A thorough investigation on the excitation wavelength dependence of the PL decay times is required to clarify this issue.

In conclusion, we demonstrated the coupling of ND with gold nanoparticles using DNA sequences as a linker. PL due to the presence of the N-V centers in the NDs was enhanced when the gold nanoparticles with various sizes were attached. The PL profile was modified in different ways when the gold nanoparticles with different plasmon resonances (different sizes) were bound to the NDs via the DNA linkers. We also demonstrated that enhancement mechanism can be deactivated by detaching the gold nanoparticles from the ND via interaction with the NdeI restriction enzyme. The approach can also be extended to other color center and metal nanoparticles, thereby providing a method for biochip and biomolecular detection.

This work was supported by a grant from the National Science Council, ROC (Grant No. NSC 99-2119-M-009-004-MY3).

[1]P. Anger, P. Bharadwaj, and L. Novotny, Phys. Rev. Lett. **96**, 113002 (2006).
[2]F. Tam, G. P. Goodrich, B. R. Johnson, and N. J. Halas, Nano Lett. **7**, 496 (2007).
[3]E. Dulkeith, A. C. Morteani, T. Niedereichholz, T. A. Klar, J. Feldmann, S. A. Levi, F. J. C. M. van Veggel, D. N. Reinhoudt, M Möller, and D. I. Gittins, Phys. Rev. Lett. **89**, 203002 (2002).
[4]G. Schneider, G. Decher, N. Nerambourg, R. Praho, M. H. V. Werts, and M. Blanchard-Desce, Nano Lett. **6**, 530 (2006).
[5]G. P. Wiederrecht, G. A. Wurtz, and J. Hranisavljevic, Nano Lett. **4**, 2121 (2004).
[6]S. M. Nie and S. R. Emory, Science **275**, 1102 (1997).
[7]P. P. Pompa, L. Martiradonna, A. Della Torre, F. Della Sala, L. Manna, M. de Vittorio, F. Calabi, R. Cingolani, and R. Rinaldi, Nat. Nanotechnol. **1**, 126 (2006).
[8]S. P. Sundararajan, N. K. Grady, N. Mirin, and N. J. Halas, Nano Lett. **8**, 624 (2008).
[9]J. S. Lee, E. V. Shevchenko, and D. V. Talapin, J. Am. Chem. Soc. **130**, 9673 (2008).
[10]K. W. Sun, J. Y. Wang, and T. Y. Ko, Appl. Phys. Lett. **92**, 153115 (2008).
[11]P. H. Chung, E. Perevedentseva, and C. L. Cheng, Surf. Sci. **601**, 3866 (2007).
[12]Y. Mita, Phys. Rev. B **53**, 11360 (1996).
[13]G. Davies, S. C. Lawson, A. T. Collins, A. Mainwood, and S. J. Sharp, Phys. Rev. B **46**, 13157 (1992).
[14]S. Schietinger, M. Barth, T. Aichele, and O. Benson, Nano Lett. **9**, 1694 (2009).
[15]See supplementary material at http://dx.doi.org/10.1063/1.3576852 for preparation method of the Au-DNA-ND assembly.
[16]T. T. B. Nguyen, H. C. Chang, and V. W. K. Wu, Diamond Relat. Mater. **16**, 872 (2007).
[17]V. Vaijayanthimala and H. C. Chang, Nanomedicine **4**, 47 (2009).
[18]Z. Gagnon, S. Senapati, J. Gordon, and H. C. Chang, Electrophoresis **29**, 4808 (2008); Z. Gagnon, S. Senapati, and H. C. Chang, *ibid.* **31**, 666 (2010).
[19]S. Basuray, S. Senapati, A. Aijian, A. R. Mahon, and H. C. Chang, ACS Nano **3**, 1823 (2009).
[20]T. R. Strick, J. F. Allemand, D. Bensimon, A. Bensimon, and V. Croquette, Science **271**, 1835 (1996).
[21]A. Mooradian, Phys. Rev. Lett. **22**, 185 (1969).
[22]J. E. Ralph, Proc. Phys. Soc. **76**, 688 (1960).
[23]G. Davies and N. B. Manson, Ind. Diamond Rev., 50 (1980).
[24]R. A. Dugdale, Br. J. Appl. Phys. **4**, 334 (1953).
[25]G. Davies, Rep. Prog. Phys. **44**, 787 (1981).
[26]F. L. Zhao, Z. Gong, S. D. Liang, N. S. Xu, S. Z. Deng, J. Chen, and H. Z. Wang, Appl. Phys. Lett. **85**, 914 (2004).
[27]M. E. Kompan, E. I. Terukov, S. K. Gordeev, S. G. Zhukov, and Yu. A. Nikolaev, Phys. Solid State **39**, 1928 (1997).